A&A 471, 265–270 (2007)
DOI: 10.1051/0004-6361:20077486

Astronomy & Astrophysics

VLT/NACO observations of the high-magnetic field radio pulsar PSR J1119-6127⋆

R. P. Mignani[1], R. Perna[2], N. Rea[3,4], G. L. Israel[5], S. Mereghetti[6], and G. Lo. Curto[7]

[1] University College London, Mullard Space Science Laboratory, Holmbury St. Mary, Dorking, Surrey, RH5 6NT, UK
e-mail: rm2@mssl.ucl.ac.uk
[2] JILA and Department of Astrophysical and Planetary Sciences, University of Colorado, 440 UCB, Boulder, 80309, USA
[3] SRON Netherlands Institute for Space Research, Sorbonnelaan 2, 3584 CA Utrecht, The Netherlands
[4] University of Sydney, School of Physics A29, NSW 2006, Australia
[5] INAF Astronomical Observatory of Rome, via di Frascati 33, 00040 Monte Porzio, Italy
[6] Istitituto di Astrofisica Spaziale, via Bassini 15, 20133 Milan, Italy
[7] European Southern Observatory, Alonso de Cordova 3107, Vitacura, Santiago, Casilla 19001 Santiago 19, Chile

Received 16 March 2007 / Accepted 13 June 2007

ABSTRACT

Context. Recent radio observations have unveiled the existence of a number of radio pulsars with spin-down derived magnetic fields in the magnetar range. However, their observational properties appear to be more similar to those of the classical radio pulsars than to the magnetars's ones.
Aims. To shed light on this puzzle we first have to determine whether the spin-down derived magnetic field values for these radio pulsars are indeed representative of the actual neutron star magnetic field or if they are polluted, e.g. by the effects of a torque from a fallback disk.
Methods. To investigate this possibility, we have performed deep IR (J, H, K_s bands) observations of one of these high magnetic field radio pulsars (PSR J1119–6127) with the ESO *VLT* to search for IR emission which can be associated with a disk.
Results. No IR emission is detected from the pulsar position down to $J \sim 24$, $H \sim 23$ and $K_s \sim 22$.
Conclusions. By comparing our flux upper limits with the predictions of fallback disk models, we have found that we can only exclude the presence of a disk with accretion rate $\dot{M} \gtrsim 3 \times 10^{16}$ g s^{-1}. This lower limit cannot rule out the presence of a substantial disk torque on the pulsar, which would then lead to overestimate the value of the magnetic field inferred from P and $\dot{P}$. We have also compared the upper limit on the IR luminosity of PSR J1119–6127 with the IR luminosities of rotation-powered pulsars and magnetars. We found that, while magnetars are intrinsically more efficient IR emitters than rotation-powered pulsars, possibly because of their higher magnetic field, the relatively low IR emission efficiency of PSR J1119–6127 suggests that it is more similar to the latters than to the former.

Key words. stars: pulsars: individual: PSR J1119–6127

1. Introduction

High-energy observations performed in the last two decades have unveiled the existence of a few unusual classes of neutron stars (NSs; see Popov 2007, for a review). The Anomalous X-Ray Pulsars (AXPs) and the Soft Gamma-Ray Repeaters (SGRs) are among them the most peculiar objects (see Woods & Thompson 2006, for a recent review). At variance with the majority of the NSs known so far, i.e. the radio pulsars, they are typically radio quiet but show X-ray pulsations at periods of a few seconds. Furthermore, the X-ray luminosity of both SGRs and AXPs largely exceeds their rotational energy ($L_X \approx 100 \times \dot{E}$), while the rotational energy of radio pulsars can easily account for their X-ray emission ($L_X \sim 0.001 \times \dot{E}$; Becker & Trümper 1997; Possenti et al. 2002). The properties of AXPs and SGRs are well explained by the magnetar model which interpretes these objects as isolated neutron stars with magnetic fields $B \sim 10^{14-15}$ G (hence dubbed magnetars), consistent with their observed spin-down with the usual vacuum dipole losses[1]. In the magnetar model, the X-ray luminosity is thought to be powered by the magnetic field decay, while radio pulsations were believed to be suppressed by processes such as the photon splitting, which inhibit pair-production cascades in magnetic fields greater than the "quantum critical field" $B_c = 4.4 \times 10^{13}$ G (Baring & Harding 1998).

This dichotomy between the two different pulsar classes – radio pulsars with $B < B_c$ on one side, and magnetars with $B > B_c$ on the other – was shaken by the discovery of radio pulsars with magnetic fields above B_c (Camilo et al. 2000). Despite having such high magnetic fields, although lower than those of the magnetars, these high-magnetic field radio pulsars (HBRPs) do not behave according to any of the known magnetars templates. First of all, *they are* radio pulsars, while pulsed radio emission has been discovered so far only in the transient magnetar XTE J1810–197 (Camilo et al. 2006). Second, only two HBRPs, PSR J1119–6127 (Gonzalez & Safi-Harb 2003) and PSR J1718–3718 (Kaspi & McLaughlin 2005), have been detected in X-rays so far, with luminosities $L_X \sim 10^{32-33}$ erg s^{-1} almost two orders of magnitude lower than those of the magnetars and smaller than their $\dot{E}$. Finally, HBRPs do not show bursting emission, either in X-rays or in γ-rays, while AXPs and SGRs instead do. These differences might be explained assuming e.g., that HBRPs are dormant transients, that their lower X-ray

⋆ Based on observations collected at the European Southern Observatory, Paranal, Chile under programme ID 076.D-0613(A).

[1] Through the paper magnetic fields are computed (in G) using the relation $B = 3.2 \times 10^{19}(P\,\dot{P})^{1/2}$, where P is the NS period (s), $\dot{P}$ is its spin-down rate (s s^{-1}).

Table 1. Summary of the *NACO J*, *H*, *K*-band observations of the PSR J1119-6127 field with the number of exposure sequences, the total number of exposures per filter, the DIT and NDIT, the average seeing and airmass.

yyyy.mm.dd	Filter	N	$N_{\rm exp}$	DIT (s)	NDIT	Seeing ($''$)	Airmass
2006.01.25	$K_{\rm s}$	1	8	20	16	0.76	1.26
2006.02.23	$K_{\rm s}$	2	30	55	3	0.66	1.30
2006.02.24	H	2	30	55	3	0.61	1.29
	J	2	30	55	3	0.88	1.27
2006.02.28	J	1	15	55	3	0.59	1.32

luminosities are a consequence of their lower magnetic fields, or simply assuming that different evolutionary paths or stages account for the different phenomenologies.

Of course, one alternative possibility is that the spin-derived magnetic field values of the HBRPs are unreliable because e.g., they are overestimated by the extra torque produced by a fossil disk formed out of residual matter from the supernova explosion. Fossil disks around isolated NSs have been invoked over the years to explain a large variey of phenomena (e.g. Michler & Dressler 1981; Lin et al. 1991; Phinney & Hansen 1993; Podsiadwolski 1993; Chatterjee et al. 2000; Alpar 2001; Menou et al. 2001; Blackman & Perna 2004; Cordes & Shannon 2006), and at least in the case of the AXP 4U 0142+61, recent *Spitzer* observations possibly revealed the presence of one of these disks (Wang et al. 2006). Thus, if HBRPs do have fossil disks, they should be detectable through deep, high-resolution IR observations. Since the IR luminosity of a hypothetical disk is expected to be larger for X-ray bright pulsars due to the flux contribution from the reprocessing of the X-ray radiation (Perna et al. 2000; Perna & Hernquist 2000), the primary candidates are obviously the HBRPs detected in X-rays.

In this work we report on the results of our recent deep IR observations of PSR J1119–6127. The pulsar was discovered in the Parkes multi-beam survey (Camilo et al. 2000) with period $P = 407$ ms and period derivative $\dot{P} \sim 4.022 \times 10^{-12}$ s s^{-1}, which give a characteristic age of ∼1600 years, a rotational energy loss $\dot{E} \sim 2.3 \times 10^{36}$ erg s^{-1}, and a magnetic field $B \sim 4.1 \times 10^{13}$ G. PSR J1119–6127 is also one of the very few pulsars with a measure of the braking index (2.9 ± 0.1; Camilo et al. 2000). X-ray emission was first detected with *Chandra* (Gonzalez & Safi-Harb 2003) which also revealed a compact pulsar wind nebula, while X-ray pulsations were discovered with *XMM-Newton* (Gonzalez et al. 2005).

The structure of the paper is as follows: IR observations and results are described in Sect. 2, while comparisons with disk models and with IR observations of other isolated NSs are discussed in Sects. 3 and 4, respectively.

2. IR observations

2.1. Observations description

IR observations of PSR J1119–6127 have been performed in Service Mode on January 25th, February 23rd, 24th and 28th 2006 with *NAos COnica* (*NACO*), an adaptive optics (AO) imager and spectrometer mounted at the fourth Unit Telescope (UT4) of the *VLT*. In order to provide the best combination between angular resolution and sensitivity, *NACO* has been operated with the S27 camera with a corresponding field of view of $28'' \times 28''$ and a pixel scale of $0\farcs027$. As a reference for the AO correction we have used the *GSC-2* star S111230317098 ($V = 13.7$), located $29\farcs5$ away from our target. Unfortunately, no suitable reference star was available within the small *NACO* S27 field of view, which makes our AO correction not optimal and more sensitive on small scale fluctuations of the atmospheric conditions. The Visual (VIS) dichroic element and wavefront sensor (4500−10 000 Å) have been used. Observations have been performed in the ESO Johnson $J(\lambda = 12\,650$ Å; $\Delta\lambda = 2500$ Å), $H(\lambda = 16\,600$ Å; $\Delta\lambda = 3300$ Å) and $K_{\rm s}(\lambda = 21\,800$ Å; $\Delta\lambda = 3500$ Å) filters.

To allow for subtraction of the variable IR sky background, each observation has been split in two sequences of short randomly dithered exposures with Detector Integration Times (DIT) of 20 and 55 s, and NDIT repetitions along each point of the dithering pattern (see Table 1). This yields a total net integration time of about 2500 s per band, per exposure sequence. For each exposure, the instrument readout mode has been selected according to the used DIT in order to minimize the read out noise. Owing to the expected faintness of the target, the DIT/NDIT combination has been modified after the $K_{\rm s}$ band observation of the first night to allow for a better signal-to-noise in the single exposures and to allow for a better hot pixels rejection.

For all our observations, the seeing conditions were on average below $0\farcs8$ and the airmass was better than 1.3, allowing for a better yield of the *NACO* adaptive optics. Sky conditions were photometric in both nights. Night (twilight flat fields) and day time calibration frames (darks, lamp flat fields) have been taken daily as part of the *NACO* calibration plan. Standard stars from the Persson et al. (1998) fields have been observed at the beginning of all nights for photometric calibration. As we expect the photometry errors to be dominated by the target's counts statistic rather than by the accuracy of the photometric calibration, we have not acquired photometric standard star fields prior to each exposure sequence.

2.2. Data reduction and analysis

The data have been processed using the ESO *NACO* pipeline[2] and the science images reduced with the produced master dark and flat field frames. For each band, and for each night, single reduced science exposures have been combined to produce cosmic-ray free and sky-subtracted images. The photometric calibration pipeline yielded average zero points of 23.03 ± 0.02 and 23.08 ± 0.03 ($K_{\rm s}$) for January 25th and February 23rd, respectively, 24.08 ± 0.04 (J) and 23.94 ± 0.04 (H) for February 24th, and 24.1 ± 0.05 (J) for February 28th. The data have been reduced independently using procedures run under the *eclipse* package[3] yielding qualitatively similar data.

As a reference for the position of PSR J1119–6127 we have used its radio coordinates $\alpha(J2000) = 11^{\rm h}19^{\rm m}14.30^{\rm s}$, $\delta(J2000) = -61°27'49\farcs5$, which have an accuracy of $0\farcs2$ (Camilo et al. 2000). The astrometry on the *NACO* image have been computed using as a reference 7 stars selected from the *2MASS* catalogue. The pixel coordinates of these stars (all non saturated and evenly

[2] http://www.eso.org/observing/dfo/quality/NACO/

[3] http://www.eso.org/projects/aot/eclipse/

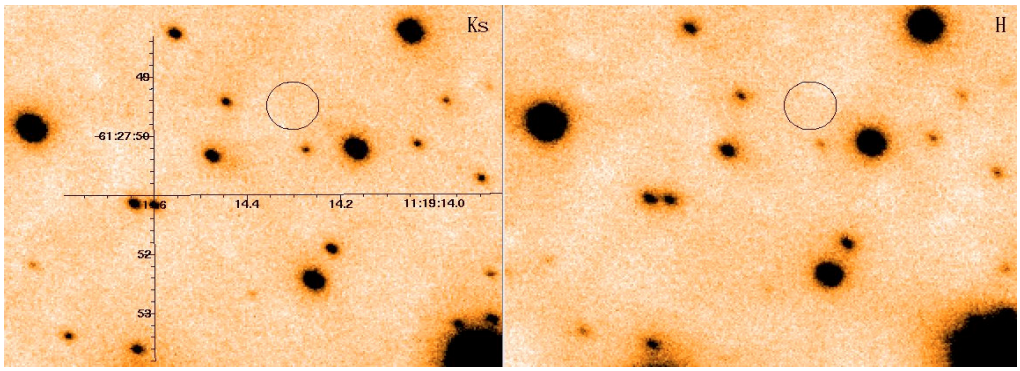

Fig. 1. 6″ × 6″ sections of the *VLT/NACO* K_s and H band images of the PSR J1119-6127 field. North to the top, East to the left. The effect of the worse AO correction (see Sect. 2.1) is recognized from the asymmetric PSF of the stars in the field. The circle (0.″3 radius) corresponds to the pulsar radio position uncertainty after accounting for the accuracy of our astrometric solution (see Sect. 2.2).

distributed in the field) have been measured by gaussian fitting their intensity profiles using the specific function of the GAIA (Graphical Astronomy and Image Analysis) tool[4] while the fit to the α, δ reference frame has been performed using the Starlink package ASTROM[5]. The rms of the astrometric solution turned out to be ≈0.″09 per coordinate. After accounting for the 0.″2 average astrometric accuracy of *2MASS*[6], the overall uncertainty to be attached to the position of our target is finally 0.″3.

2.3. Results

Figure 1 shows the K_s and H band images of the PSR J1119–6127 field with the computed pulsar radio position overlaid. No potential counterpart is detected at the expected position, with the closest object being detected ∼1σ away from the edge of the error circle. The same is true also for the J band image. We thus conclude that both the pulsar and its putative disk are undetected in each of the three observing bands down to estimated limiting magnitudes of $J \sim 24$, $H \sim 23$ and $K_s \sim 22$. At the same time, no diffuse emission is recognized which can be possibly associated with the X-ray pulsar wind nebula detected by *Chandra* (Gonzalez & Safi-Harb 2003).

3. Discussion

3.1. Comparison with disk models

We have used the derived IR flux upper limits to constrain the range of parameters that a hypothetical fossil disk around the pulsar could have. If a disk were indeed present and interacting with the pulsar magnetosphere, then, as mentioned in Sect. 1 and detailed below, the B field inferred from P and $\dot{P}$ could be largely overestimated. The torque exterted by a disk on the star magnetosphere can be written as (e.g. Menou et al. 2001) $\dot{J}_{\rm disk} = I\dot{\Omega} \sim -2\dot{M}R_{\rm in}^2\Omega$, where $\dot{M}$ is the disk accretion rate, $R_{\rm in}$ is the disk inner radius, and $\Omega = 2\pi/P$ is the angular frequency of the pulsar. The fact that PSR J1119–6127 is detected in radio implies that $R_{\rm in}$ cannot be smaller than the light cylinder radius $R_{\rm lc} = c/\Omega$ (e.g. Illarionov & Sunyaev 1975). On the other hand, if the inner radius of the disk were outside of the light cylinder, where the magnetic field lines are open, no efficient torque could operate. Therefore, in the following analysis we consider only the case $R_{\rm in} = R_{\rm lc}$, which yields a torque $\dot{J}_{\rm disk} = -2\dot{M}c^2/\Omega$ or, equivalently, an energy loss (in modulus) $\dot{E}_{\rm disk} \sim 2\dot{M}c^2 = 2 \times 10^{37}\ \dot{M}/(10^{16}{\rm g\ s^{-1}})$ erg s^{-1}. Under these conditions, the total energy loss of the pulsar, accounting for both the dipole and the disk torque components, is given by $\dot{E} = \dot{E}_{\rm dip} + \dot{E}_{\rm disk} \sim B^2\Omega^4R^6/6c^3 + 2\dot{M}c^2$, where R is the radius of the star. Clearly, if $\dot{E}_{\rm disk} \gtrsim \dot{E}_{\rm dip}$, the value of B that is inferred from P and $\dot{P}$, i.e. assuming $\dot{E} = \dot{E}_{\rm dip}$, could be largely overestimated. In the case of PSR J1119–6127, a fallback disk with accretion rate of the order of 10^{15} g s^{-1} could account for the entire energy loss of the pulsar ($\dot{E} \sim 2.3 \times 10^{36}$ erg s^{-1}), even without the contribution of dipole losses, which would be the case for a very low magnetic field. We thus take $\dot{M} \sim 10^{15}$ g s^{-1} to be the accretion rate corresponding to the maximum torque that could be produced by a hypothetical disk.

We have simulated the disk IR spectrum using the disk model developed by Perna et al. (2000), which takes into account the contribution to the disk IR emission due to both viscous dissipation and reprocessing of the X-ray radiation from the pulsar. The spectra have been renormalized for the distance d to PSR J1119–6127. Camilo et al. (2000) reported $d = 2.4$–8 kpc, while Gonzalez & Safi-Harb (2003), based on the measured extinction per unit distance in the pulsar direction, estimated $d = 5.4$–12.6 kpc. Most likely, the pulsar is not further than 8 kpc, according to its location with respect the Carina spiral arm (Camilo et al. 2000). In the following we report our results as a function of $D_6 = d/(6$ kpc$)$. Figure 2 shows the modelled disk IR spectra computed for two different values of the disk accretion rate $\dot{M}$ compared to the observed IR flux upper limits. In particular, we show the predicted flux corresponding to the maximum value of $\dot{M}$ that would make the disk emission compatible with the current limits, as well as the flux corresponding to the maximum value of $\dot{M}$ compatible with the spin down rate of the pulsar.

We find that our limits only rule out disks with $\dot{M} \gtrsim 3 \times 10^{16}\ D_6^2$ g s^{-1}, i.e. well above the value of 10^{15} g s^{-1} corresponding to the case of maximum allowed disk torque. Therefore, we cannot exclude with the current observations that the magnetic field derived from the pulsar spin-down, under the assumption of a purely vacuum dipole energy loss, be overestimated due to pollution by a disk torque. We note that, given the low X-ray luminosity of PSR J1119–6127, $L_{0.5-10\ {\rm keV}} = 5.5^{+10}_{-3.3} \times 10^{32} \times D_6^2$ erg s^{-1} (Gonzalez & Safi-Harb 2003), the contribution to the disk IR emission due to the X-rays reprocessing is so low that it becomes comparable with that due to viscous dissipation in the disk only for $\dot{M} \lesssim 5 \times 10^{15}\ D_6^2$ g s^{-1}. For this reason, the derived IR flux upper limits for PSR J1119–6127 are less stringent

[4] star-www.dur.ac.uk/~pdraper/gaia/gaia.html
[5] http://star-www.rl.ac.uk/Software/software.htm
[6] http://spider.ipac.caltech.edu/staff/hlm/2mass/

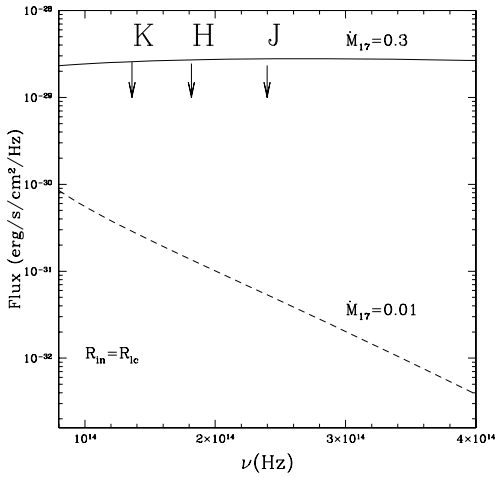

Fig. 2. Expected IR spectrum of a fallback disk of inner radius $R_{\rm in} = R_{\rm lc}$ and two values of the disk accretion rate $\dot{M}$: *solid line*: maximum value of $\dot{M}$ compatible with the IR limits; *dashed line*: maximum value of $\dot{M}$ compatible with the pulsar's spin down rate. The IR flux upper limits have been corrected for the interstellar extinction applying the relations of Fitzpatrick (1999) for $A_V = 5$, as derived from the X-ray absorption $N_{\rm H} = 9^{+5}_{-3} \times 10^{21}$ cm^{-2} (Gonzalez & Safi-Harb 2003) and the relation $A_V = N_{\rm H}/1.79 \times 10^{21}$ atoms cm^{-2} mag^{-1} (Predhel & Schmitt 1995).

in ruling out a fallback disk at the light cylinder with respect to similarly deep upper limits obtained for the AXPs which, instead, have a much higher X-ray luminosity. Indeed, an X-ray luminosity higher by a factor 100 would raise the disk IR emission much closer to our present upper limits.

We have seeked for other evidence which might indirectly unveil the existence of a fallback disk and the effect of its torque on the pulsar's spin down. In principle, a torque from a fallback disk should leave a signature in the pulsar timing by increasing the level of the timing noise. In the case of PSR J1119–6127, the level of the radio timing noise does not show any clearly anomalous excess which might be associated with the effect of an acting disk torque, and it seems apparently consistent with the level expected for its high $\dot{P}$ (Arzoumanian et al. 1994). However, we note that the magnitude of the effect would depend on the actual value of the disk torque, which is obviously unknown, and it might be confused with the underlying timing noise. In any case, the timing analysis can in no way rule out that the pulsar's spin down might have been affected by a disk torque in the past.

3.2. Comparison with other NSs

For the estimated ranges of distance and $N_{\rm H}$ (see previous section), our flux upper limits yield for PSR J1119–6127 a K-band IR luminosity $L_K \leq 6.6^{+11}_{-4} \times 10^{30} \times D_6^2$ erg s^{-1}. We have compared this upper limit with the IR luminosities of different classes of isolated NSs. We caveat here that the nature of the IR emission may be different across the whole sample. For instance, in the case of rotation-powered pulsars, the IR emission is thought to be produced in the NS magnetosphere, as shown by their power-law spectra (e.g. Shibanov et al. 2003), while in the case of the magnetars it might be produced by an X-ray irradiated, (though passive), fallback disk, by the magnetic field decay, or by curvature radiation in the magnetars' coronae (Beloborodov & Thomspon 2007). Nevertheless, comparing the IR properties of different classes of isolated NSs can still be useful to unveil similarities and diversities which can be indeed ascribed to different emission processes and thus be used to disantangle, e.g. magnetospheric and disk emitters.

Table 2 summarizes the IR flux measurements for all the isolated NSs with an IR counterpart, i.e. rotation-powered pulsars and magnetars. In order to make a consistent comparison with rotation-powered pulsars, which are persistent emitters, for the magnetars we have selected only IR flux measurements taken when the X-ray source was as close as possible to quiescence. We have include in our compilation also the AXP 1RXS J170849–400910, although its IR identification has not been confirmed yet (Safi-Harb & West 2005; Durant & van Kerkwijk 2006; Rea et al. 2007a), hence we did not consider it in the following analysis. The proposed identification of 1E 1841−045 (Wachter et al. 2004) has been discarded by high-resolution IR observations (Durant 2005). No IR emission has been detected so far from the X-ray Dim Isolated NSs (XDINSs; Mignani et al. 2007; Lo Curto et al. 2007; Rea et al. 2007b) and from any compact central objects (CCOs) in SNRs (Wang et al. 2007; Fesen et al. 2006).

For each object we have computed its IR luminosity either in the $K_{\rm s}$ or in the K band, as we estimate the error due to the passband correction to be below ∼0.1 mag, i.e. fully acceptable for the goals of our analysis. For Vela and Geminga, we have extrapolated their K-band magnitudes from the IR colors. Passband transformations between different K-band filters have been neglected. The flux conversion from the *HST*/*NICMOS* passbands to the Johnson's ones has been applied using the *NICMOS* Units Conversion tool[7].

For the rotation-powered pulsars, distance values have been taken either from the available radio/optical parallaxes or from the radio dispersion measure (Cordes & Lazio 2002)[8]. For the magnetars we have used either the distances of the parental stellar clusters or of the associated supernova remnants, or the distances inferred from the $N_{\rm H}$ (see Table 2 and references therein). For the interstellar extinction correction we have applied the relations of Fitzpatrick (1999) using as a reference either the measured A_V or the value derived from the $N_{\rm H}$ recomputed from our X-ray spectral fits and the relation of Predehl & Schmitt (1995). For the magnetars we have fitted an absorbed power-law plus a blackbody model (see Tiengo et al. 2005; Rea et al. 2004, 2005; Woods et al. 2004; Patel et al. 2003; Morii et al. 2003; Mereghetti et al. 2004, for further details on the single observations) over the spectral range 2−10 keV. All the $N_{\rm H}$ values have been computed assuming solar abundances from Anders & Grevesse (1989). Although the reference A_V have been obtained with different methods, this does not affect significantly our estimates of the IR luminosity, expecially in the K-band where the effects of the interstellar extinction are lower. The overall IR luminosity errors take into account the measured photometric errors as well as all the uncertainties on the isolated NS distance and on the interstellar extinction correction, all reported in Table 2.

3.3. Results

In the left panel of Fig. 3 we have plotted the computed IR luminosities L_K for all the isolated NSs in Table 2, and the upper limit for PSR J1119–6127, as a function of the NSs rotational energy loss $\dot{E}$. From this plot we clearly see that the rotation-powered pulsars and the magnetars cluster in quite distinct regions of the diagram. In particular, PSR J1119–6127 is definitely closer to

[7] http://www.stsci.edu/hst/nicmos/tools/
[8] http://rsd-www.nrl.navy.mil/7213/lazio/ne_model/

Table 2. Summary of the IR fluxes measurements for all types of isolated NSs with an identified IR counterpart i.e. rotation-powered pulsars (rows 1−5) and magnetars (rows 6−11). The columns give the observed J, H, K, K_s magnitudes (an hyphen stands for non-detection, values in italics have been extrapolated), the distance, and the interstellar extinction A_V either derived from existing optical measurements (O) or from the N_H derived from the fits to the X-ray spectra (X) by using the relation of Predehl & Schmitt (1995). K-band flux values in italics have been derived from the extrapolation of the J and H-band fluxes.

NS Name	J	H	K	K_s	d(kpc)	A_V	Ref.
Crab	14.8 ± 0.05	14.3 ± 0.05	13.8 ± 0.05	–	1.730 ± 0.28	1.62 (O)	1, 2, 3
PSR B1509–58	–	20.6 ± 0.20	–	19.4 ± 0.1	4.181 ± 0.60	4.8 (O)	4, 2, 5
Vela	22.7 ± 0.10	22.0 ± 0.16	*21.3 ± 0.4*	–	$0.294^{+0.019}_{-0.017}$	0.20 (O)	6, 7, 8
PSR B0656+14*	24.4 ± 0.10	23.2 ± 0.08	22.6 ± 0.13	–	$0.288^{+0.033}_{-0.027}$	0.09 ± 0.06(O)	9, 10, 11
Geminga*	25.1 ± 0.10	24.3 ± 0.10	*23.4 ± 0.4*	–	$0.157^{+0.059}_{-0.034}$	0.12 ± 0.09(O)	9, 12, 13
4U 0142+61**	–	–	19.7 ± 0.05	20.1 ± 0.08	≥5	5.1 (X)	14, 15
1E 1048.1–5937	21.7 ± 0.30	20.8 ± 0.30	–	21.3 ± 0.30	3 ± 1	6.1 (X)	16, 17, 15
1RXS J170849–400910[x]	20.9 ± 0.10	18.6 ± 0.10	–	18.3 ± 0.10	5	7.8 (X)	18, 15
XTE J1810–197	–	22.0 ± 0.10	–	20.8 ± 0.10	4 ± 1[+]	5.1 (X)	19, 20, 15
1E 2259+586	–	–	–	21.7 ± 0.20	3.0 ± 0.5	5.7 ± 0.1 (O)	21, 22, 23
SGR 1806–20	–	–	–	20.1 ± 0.14	15.1 ± 1.6	29 ± 2 (O)	24, 25, 26

(1) Sollerman (2003); (2) radio dispersion measure, Cordes & Lazio (2002); (3) Sollerman et al. (2000); (4) Kaplan & Moon (2006); (5) Lortet et al. (1987); (6) Shibanov et al. (2003); (7) radio parallax, Dodson et al. (2003); (8) Mignani et al. (2003); (9) Koptsevich et al. (2001); (10) radio parallax, Brisken et al. (2003); (11) Pavlov et al. (1997); (12) optical parallax, Caraveo et al. (1996); (13) Kargaltsev et al. (2005); (14) Hulleman et al. (2004); (15) present work; (16) Wang & Chakrabarty (2002); (17) Gaensler et al. (2005); (18) Israel et al. (2003); (19) Israel et al. (2004); (20) Rea et al. (2004); (21) Hulleman et al. (2001); (22) Kothes et al. (2002); (23) Woods et al. (2004); (24) Israel et al. (2005); (25) Mc Clure-Griffiths & Gaensler (2005); (26) Eikenberry et al. (2004); * magnitudes refer to the *HST/NICMOS* filters *110W*, *160W*, *187W*, which overlap the J, H and K passbands; ** K and K_s magnitudes have been taken at different epochs; [x] IR counterpart still to be confirmed (Safi-Harb & West 2005; Durant & van Kerkwijk 2006; Rea et al. 2007a); [+] revised downward to 2.5 kpc (Gotthelf & Halpern 2005).

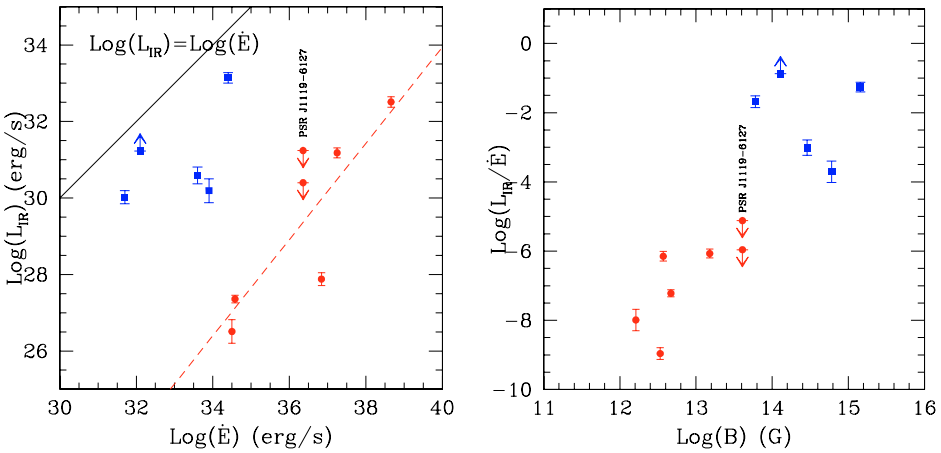

Fig. 3. *left panel*: measured K-band luminosities for all the isolated NSs listed in Table 2 as a function of the NSs rotational energy loss $\dot{E}$. For J1119–6127 (labelled in the figures) we have plotted the IR luminosity upper limits corresponding to the most extreme distance/absorption values. For 4U 0142+61 we have plotted the IR luminosity lower limit corresponding to a lower limit on the source distance of 5 kpc (Hullemann et al. 2004). Red filled circles and blue filled squares indicate rotation-powered pulsars and magnetars, respectively. The red dashed line corresponds to the linear fit for rotation-powered pulsars while the solid line shows the limit case Log(L_K) = Log($\dot{E}$). *Right panel*: the derived IR efficiencies, defined as the ratio between L_K and $\dot{E}$, as a function of the dipole magnetic field B inferred from the NS spin down. Timing parameters have been taken from the ATNF Pulsar Database (`http://www.atnf.csiro.au/research/pulsar/psrcat`) for rotation-powered pulsars, and from Woods & Thompson (2006) for the magnetars. For both 1E 1048–5937 and SGR 1806–20 we have taken as a reference the average $\dot{P}$ value.

the group of the rotation-powered pulsars than to the magnetars one, which would suggest its connection with the formers rather than with the latters.

From a general point of view, it is clear that there is no substantial difference between the IR luminosity of the magnetars and that of the young (≤5000 years) rotation-powered pulsars (Crab and PSR B1509–58), which have all luminosities $L_K \sim 10^{30}$–10^{32} erg s^{-1} to be compared with $L_K \sim 10^{26}$–10^{28} erg s^{-1} of the older rotation-powered pulsars (Vela, PSR B0656+14 and Geminga). For the rotation-powered pulsars Fig. 3 shows that the IR luminosity correlates rather well with the rotational energy loss, with $L_K \propto \dot{E}^{1.3\pm0.04}$. This correlation is similar to the one found for the optical luminosity, i.e. $L_{opt} \propto \dot{E}^{1.6\pm0.2}$ (see, e.g. Kramer 2004), which confirms that the IR emission of rotation-powered pulsars, like the optical one, is mostly magnetospheric.

Instead, for the magnetars the scatter of the points does not allow to recognize a correlation between L_K and $\dot{E}$. However, if the magnetars' IR emission were also powered by their rotational energy they would be much more efficient IR emitters than the rotation-powered pulsars, with IR luminosities much closer to their $\dot{E}$. In particular, we note that, if the distance lower limit of 5 kpc is confirmed, the IR luminosity of 4U 0142+61 could be comparable to its its $\dot{E}$, making it the intrinsically more luminous magnetar. This intrinsically larger IR output could be

explained by the presence of an additional source of emission which, at least in the case of 4U 0142+61, might be identified with a possible fossil disk (Wang et al. 2006). The same might be true also for the other magnetar with the highest IR luminosity (SGR 1806–20), while for the others the presence of a surrounding fallback disk appears less compelling. Alternatively, it is possible that the IR emission of magnetars is powered, as it is in the X-rays, by the star magnetic field rather than by its rotation. We have plotted in the right panel of Fig. 3 the IR emission efficiency as a function of the dipole magnetic field B. Despite the scatter of the points, it is clear that the magnetic field does imply a larger IR emission efficiency for the magnetars than for the rotation-powered pulsars. We thus speculate that, although the contribution of a disk cannot be a priori ruled out, the IR emission of the magnetars is substantially driven by the magnetic field. In particular, we note that with a magnetic field $B \sim 4.1 \times 10^{13}$ G, one might expect for PSR J1119–6127 a magnetar-like IR emission efficiency, while it is at least one order of magnitude lower. This makes PSR J1119–6127, once again, more similar to the rotation-powered pulsars than to the magnetars. This might suggest that the actual magnetic field of PSR J1119–6127 is lower than the measured one and that a torque from a disk might have indeed affected the pulsar's spin down. However, we note that, given the disk accretion rate compatible with the maximum torque and the low X-ray luminosity of the pulsar (see Sect. 3.1), the contribution of such a disk to the total IR flux would likely be low enough for the pulsar IR emission to be dominated by the magnetospheric component, as in the classical, rotation-powered radio pulsars.

4. Conclusions

We have reported on deep IR observations performed with the ESO *VLT* to constrain the presence of a fallback disk around the high magnetic field radio pulsar PSR J1119–6127. No IR emission has been detected at the pulsar's position down to limiting magnitudes of $J \sim 24$, $H \sim 23$ and $K_s \sim 22$. These upper limits have been compared with the expected IR spectrum emitted from a fallback disk, which we have computed using the disk models of Perna et al. (2000). We have found that the current flux upper limits only rule out a fallback disk with $\dot{M} \gtrsim 3 \times 10^{16}$ g s^{-1}. However, a disk with an accretion rate of $\sim 10^{15}$ g s^{-1} can still account for the rotation energy loss of the pulsar, hence we cannot yet confirm or exclude that the pulsar experiences an extra torque produced by a fallback disk, and that the value of the magnetic field inferred from P and $\dot{P}$ is thus overestimated. We have also compared the upper limit on the IR luminosity of PSR J1119–6127 with the measured IR luminosities of rotation-powered pulsars and magnetars. While magnetars are intrinsically more efficient IR emitters than rotation-powered pulsars, probably because of their higher magnetic field, we have found that the relatively low IR emission efficiency of PSR J1119–6127 makes it more similar to the latters than to the formers. Although not strictly compelling, this might be an indication of a magnetic field actually lower than the measured one.

Acknowledgements. R.P.M. thanks S. Zane for her comments and suggestions. N.R. is supported by an NWO Post-doctoral Fellowship and a Short Term Visiting Fellowship awarded by the University of Sydney.

References

Alpar, M. A. 2001, ApJ, 554, 1245
Anders, E., & Grevesse, N. 1989, Geochim. Cosmochim. Acta, 53, 197
Arzoumanian, Z., Nice, D. J., Taylor, J. H., & Thorsett, S. E. 1994, ApJ, 422, 671
Baring, M. G., & Harding, A. K. 1998, ApJ, 507, L55
Beloborodov, A. M., & Thompson, C. 2007, ApJ, 657, 967
Blackman, E., & Perna, R. 2004, ApJ, 601, L71
Brisken, W. F., Thorsett, S. E., Golden, A., & Goss, W. M. 2003, ApJ, 593, L89
Camilo, F., Kaspi, V. M., Lyne, A. G., et al. 2000, ApJ, 541, 367
Camilo, F., Ransom, S. M., Halpern, J. P., et al. 2006, Nature, 442, 892
Caraveo, P. A., Bignami, G. F., Mignani, R., & Taff, L. G. 1996, ApJ, 461, L91
Dodson, R., Legge, D., Reynolds, J. E., & McCulloch, P. M. 2003, ApJ, 596, 1137
Chatterjee, P., Hernquist, L., & Narayan, R. 2000, ApJ, 534, 373
Cordes, J. M., & Lazio, T. J. W. 2002 [arXiv:astro-ph/0207156]
Cordes, J. M., & Shannon, R. M. 2006, ApJ, submitted [arXiv:astro-ph/0605145]
Durant, M. 2005, ApJ, 632, 563
Durant, M., & van Kerkwijk, M. 2006, ApJ, 648, 534
Eikenberry, S. S., Matthews, K., LaVine, J. L., et al. 2004, ApJ, 616, 506
Gaensler, B. M., McClure-Griffiths, N. M., Oey, M. S., et al. 2005, ApJ, 620, L95
Gonzalez, M., & Safi-Harb, S. 2003, ApJ, 591, L143
Gonzalez, M. E., Kaspi, V. M., Camilo, F., Gaensler, B. M., & Pivovaroff, M. J. 2005, ApJ, 630, 489
Gotthelf, E. V., & Halpern, J. P. 2005, ApJ, 632, 1075
Gotthelf, E. V., Halpern, J. P., Buxton, M., & Bailyn, C. 2004, ApJ, 605, 368
Hulleman, F., Tennant, A. F., van Kerkwijk, M. H., et al. 2001, ApJ, 563, L49
Hulleman, F., van Kerkwijk, M. H., & Kulkarni, S. R. 2004, A&A, 416, 1037
Illarionov, A. F., & Sunyaev, R. A. 1975, A&A, 39, 185
Kothes, R., Uyaniker, B., & Yar, A. 2002, ApJ, 576, 169
Israel, G. L., Covino, S., Perna, R., et al. 2003, ApJ, 589, L93
Israel, G. L., Rea, N., Mangano, V., et al. 2004, ApJ, 603, L97
Israel, G., Covino, S., Mignani, R., et al. 2005, A&A, 438, L1
Kaspi, V., & McLaughlin, M. 2005, ApJ, 618, L41
Kargaltsev, O. Y., Pavlov, G. G., Zavlin, V. E., & Romani, R. W. 2005, ApJ, 625, 307
Koptsevich, A. B., Pavlov, G. G., Zharikov, S. V., et al. 2001, A&A, 370, 1004
Lo Curto, G., Mignani, R. P., & Perna, R., & Israel, G. L. 2007, A&A, accepted [arXiv:0707.0516]
Lin, D. N. C., Woosley, S. R., & Bodenheimer, P. H. 1991, Nature, 353, 827
Lortet, M. C., Georgelin, Y. P., & Georgelin, Y. M. 1987, A&A, 180, 65
McClure-Griffiths, N. M., & Gaensler, B. M. 2005, ApJ, 630, L161
Menou, K., Perna, R., & Hernquist, L. 2001, ApJ, 554, L63
Mereghetti, S., Tiengo, A., Stella, L., et al. 2004, ApJ, 608, 427
Michler, F. C., & Dessler, A. J. 1981, ApJ, 251, 654
Mignani, R. P., De Luca, A., Kargaltsev, O., et al. 2003, ApJ, 594, 419
Mignani, R. P., Bagnulo, S., De Luca, A., et al. 2007, Ap&SS, 308, 203
Morii, M., Sato, R., Kataoka, J., & Kawai, N. 2003, PASJ, 55, L45
Patel, S. K., Kouveliotou, C., Woods, P. M., et al. 2003, ApJ, 587, 367
Pavlov, G. G., Welty, A. D., & Cordova, F. A. 1997, ApJ, 489, L75
Perna, R., & Hernquist, L. 2000, ApJ, 544, L57
Perna, R., Hernquist, L., & Narayan, R. 2000, ApJ, 541, 344
Phinney, E. S., & Hansen, B. M. S. 1993, in Planets around pulsars, ed. J. A. Philips, S. E. Thorsett, & S. R. Kulkarni (San Francisco: ASP), ASP Conf. Ser., 36, 371
Podsiadlowski, P. 1993, in Planets around pulsars, ed. J. A. Philips, S. E. Thorsett, & S. R. Kulkarni (San Francisco: ASP), ASP Conf. Ser., 36, 149
Popov, S. 2007, Particles and Nuclei, Letters [arXiv:astro-ph/0610593]
Predehl, P., & Schmitt, J. H. M. M. 1995, A&A, 293, 889
Rea, N., Testa, V., Israel, G. L., et al. 2004, A&A, 425, L5
Rea, N., Oosterbroek, T., Zane, S., et al. 2005, MNRAS, 361, 710
Rea, N., Israel, G. L., Oosterbroek, T., et al. 2007a, Ap&SS, 308, 505
Rea, N., Torres, M., Jonker, P., et al. 2007b, MNRAS, accepted [arXiv:0705.3717]
Safi-Harb, S., & West, J. 2005, Adv. Sp. Res., 35, 1172
Shibanov, Yu. A., Koptsevich, A. B., Sollerman, J., & Lundqvist, P. 2003, A&A, 406, 645
Sollerman, J. 2003, A&A, 406, 639
Sollerman, J., Lundqvist, P., Lindler, D., et al. 2000, ApJ, 537, 861
Tiengo, A., Mereghetti, S., Turolla, R., et al. 2005, A&A, 437, 997
Wachter, S., Patel, S., Kouveliotou, C., et al. 2004, ApJ, 615, 887
Wang, Z., & Chakrabarty, D. 2002, ApJ, 579, L33
Wang, Z., Chakrabarty, D., & Kaplan, D. L. 2006, Nature, 440, 772
Wang, Z., kaplan, D., & Chakrabarty, D. 2007, ApJ, 655, 261
Woods, P. M., & Thompson, C. 2006, in Compact Stellar X-ray Sources, ed. W. H. G. Lewin, & M. van der Klis, 39, 547
Woods, P. M., Kaspi, V. M., Thompson, C., et al. 2004, ApJ, 605, 378